

High spin states in ^{97}Rh and ^{103}Rh

G. Kajrys, S. Landsberger,* and S. Monaro

Laboratoire de Physique Nucléaire, Université de Montréal, Montréal, Québec, Canada H3C3J7

(Received 12 July 1983)

High spin states in ^{97}Rh and ^{103}Rh have been studied via the $^{94,100}\text{Mo}(^6\text{Li},3n\gamma)$ reaction using in-beam gamma ray spectroscopy techniques. Two cascades based on the $\frac{1}{2}^-$ ground state and the lowest $\frac{9}{2}^+$ state are attributed to ^{103}Rh . Two cascades based on a proposed $\frac{13}{2}^+$ level are attributed to ^{97}Rh . Excitation function and angular distribution measurements are used to assign spin values to many of the levels.

NUCLEAR REACTIONS $^{94,100}\text{Mo}(^6\text{Li},3n\gamma)^{97,103}\text{Rh}$, $E=22-34$ MeV. Measured E_γ , γ - γ coincidences, γ -ray angular distributions. ^{97}Rh , ^{103}Rh deduced levels, J^π ; enriched targets, Ge(Li) detectors.

I. INTRODUCTION

While our knowledge on the odd-mass neutron-rich Tc and Rh nuclei (for which $N \geq 50$) is far from complete, many interesting features and similarities have already emerged. For example, in the $^{93-99}\text{Tc}$ nuclei, positive parity bands connected by predominantly $E2$ transitions have been observed based on the $\frac{9}{2}^+$ ground state. The positions of the lowest (yrast) $\frac{13}{2}^+$, $\frac{17}{2}^+$ and $\frac{21}{2}^+$ states in these nuclei correspond closely in energy with the 2^+ , 4^+ , and 6^+ states in the corresponding $(A-1)$ $^{92-98}\text{Mo}$ nuclei.¹ Similar bands have been proposed also in ^{99}Rh and ^{101}Rh .² Here, however, the positions of the $\frac{13}{2}^+$, $\frac{17}{2}^+$, and $\frac{21}{2}^+$ states are consistently higher in energy than the corresponding 2^+ , 4^+ , and 6^+ states in ^{98}Ru and ^{100}Ru . This lack of correspondence is even more pronounced for ^{103}Ag and ^{102}Pd .¹ Indeed, whereas the 2^+ , 4^+ , and 6^+ states of the even-even $N=54$ and $N=56$ isotones show a fairly smooth decrease in energy with increasing Z , the $\frac{13}{2}^+$, $\frac{17}{2}^+$, and $\frac{21}{2}^+$ states of the odd- A nuclei remain almost static in energy relative to each other. Recently the existence of a negative parity band in ^{97}Tc (Ref. 3), ^{99}Rh , and ^{101}Rh (Ref. 2) has been established. The $\frac{5}{2}^-$, $\frac{9}{2}^-$, $\frac{13}{2}^-$, and $\frac{17}{2}^-$ states of these bands are considerably lower in energy than the 2^+ , 4^+ , 6^+ , and 8^+ states in the neighboring even-even nuclei. However, these levels do show a gradual lowering of excitation energy with increasing A as in the even-even nuclei.

Additionally, several states in the odd- A Tc and Rh nuclei show rapid changes in energy with increasing mass number. In the Tc nuclei the lowest $\frac{7}{2}^+$ and $\frac{5}{2}^+$ states drop sharply in energy and the $\frac{9}{2}^+$, $\frac{7}{2}^+$, $\frac{5}{2}^+$ level ordering observed in $^{97-101}\text{Tc}$ reverses itself in ^{103}Tc and has been proposed⁴ as the onset of a large permanent deformation at $N=60$. While the $\frac{7}{2}^+$ state in ^{99}Rh drops steeply in energy to become the ground state in ^{105}Rh , the known $\frac{5}{2}^+$ state is relatively static.

Clearly these features should be explainable in a sys-

tematic fashion, but many gaps still exist for a meaningful comparison to be made. In particular, little has been published on the high-spin states of ^{103}Rh and ^{97}Rh . In this work we wish to report on such states populated via the $^6\text{Li},3n$ reaction. The low lying $\frac{5}{2}^-$, $\frac{3}{2}^-$ doublet of states¹ in ^{103}Rh is similar to that observed in ^{101}Rh , so that we might expect a similar structure, while only positive-

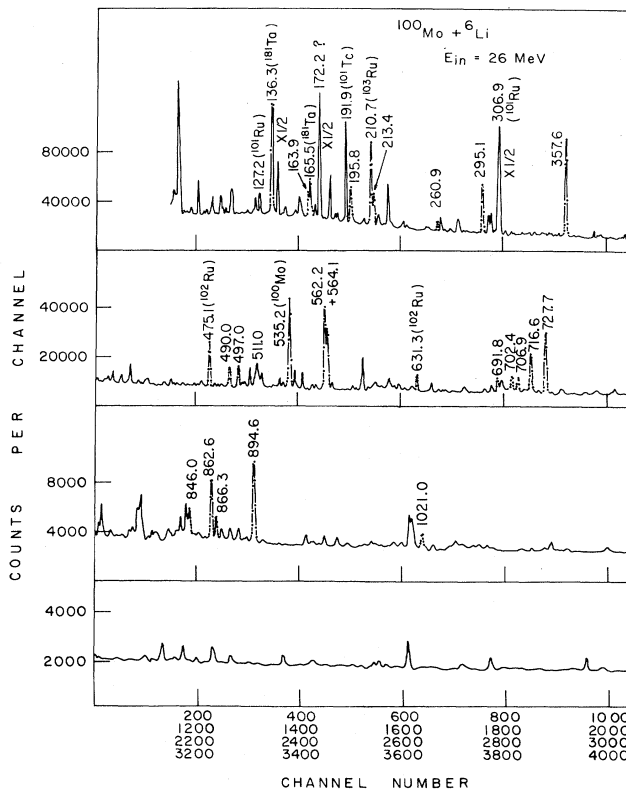


FIG. 1. A Ge(Li) spectrum from the $^{100}\text{Mo}+^6\text{Li}$ reaction at 26 MeV bombarding energy. Labeled peaks belong to ^{103}Rh unless otherwise indicated. Energies are in keV.

parity low-lying states have been clearly identified⁵ in ⁹⁷Rh so that some intermediate structure between ⁹⁵Rh and ⁹⁹Rh might be expected for ⁹⁷Rh.

II. EXPERIMENTAL PROCEDURES

Experimental procedures and data reduction techniques were identical to those reported elsewhere² and only the essential details will be outlined here. Targets of isotopically enriched ($\sim 97\%$) ⁹⁴Mo and ¹⁰⁰Mo in the form of metallic rolled foils ($t \approx 10$ mg/cm²) were bombarded with the ⁶Li beam from the Université de Montréal EN tandem Van de Graaff accelerator and, where energies higher than those obtainable in Montreal were needed, with the Chalk River Nuclear Laboratory MP tandem accelerator. In-beam gamma ray singles spectra were obtained with a 72 cm³ Ge(Li) detector, having a resolution of 2.1 keV at 1.33 MeV, placed 15 cm from the target at 90° to the incoming beam. Excitation functions of gamma rays up to 1.5 MeV in energy were measured in 2 MeV steps between 22 and 34 MeV bombarding energy.

A typical spectrum taken at 26 MeV bombarding energy and with the ¹⁰⁰Mo target is shown in Fig. 1. From the yield of the 357 keV, $\frac{5}{2}^- \rightarrow \frac{1}{2}^-$ transition in ¹⁰³Rh, a bombarding energy of 25 MeV was chosen to carry out the gamma-gamma coincidence and angular distribution experiments. For the more neutron deficient ⁹⁷Rh, using the yield of the 265.3 keV, $\frac{7}{2}^+ \rightarrow \frac{9}{2}^+$ transition, a corre-

sponding energy of 32 MeV was selected. To help identify reaction products, background spectra were recorded after each irradiation. As expected, the αn , pn, p2n, and p3n reaction channels and their respective decay products accounted for a large part of the in-beam and out of beam spectra. Because of the higher energies needed to populate states in ⁹⁷Rh, the accurate analysis of transitions assigned to ⁹⁷Rh proved to be difficult due to a large number of close-lying background lines. This difficulty did not occur for the majority of transitions assigned to ¹⁰³Rh.

Gamma-gamma coincidence measurements were performed using two Ge(Li) detectors at 55° and -90° to the beam axis and having 2.1 keV resolution at 1.33 MeV. Standard fast discriminator timing techniques were employed to achieve a prompt coincidence timing resolution of about 10 ns. Coincidence data, recorded event by event onto magnetic tape, were subsequently analyzed to obtain gamma-ray spectra in coincidence with selected peaks and background gates. Some examples of the gamma-gamma coincidence spectra are shown in Fig. 2.

Angular distribution measurements were carried out with the Ge(Li) counter placed 20 cm from the target and gamma ray spectra were recorded every 15° between 0° and 90° to the beam direction. The total incident charge together with the total counts recorded by a 12.5 cm \times 12.5 cm NaI(Tl) monitor detector placed at -90° to the beam direction served as the normalization for each recorded spectrum.

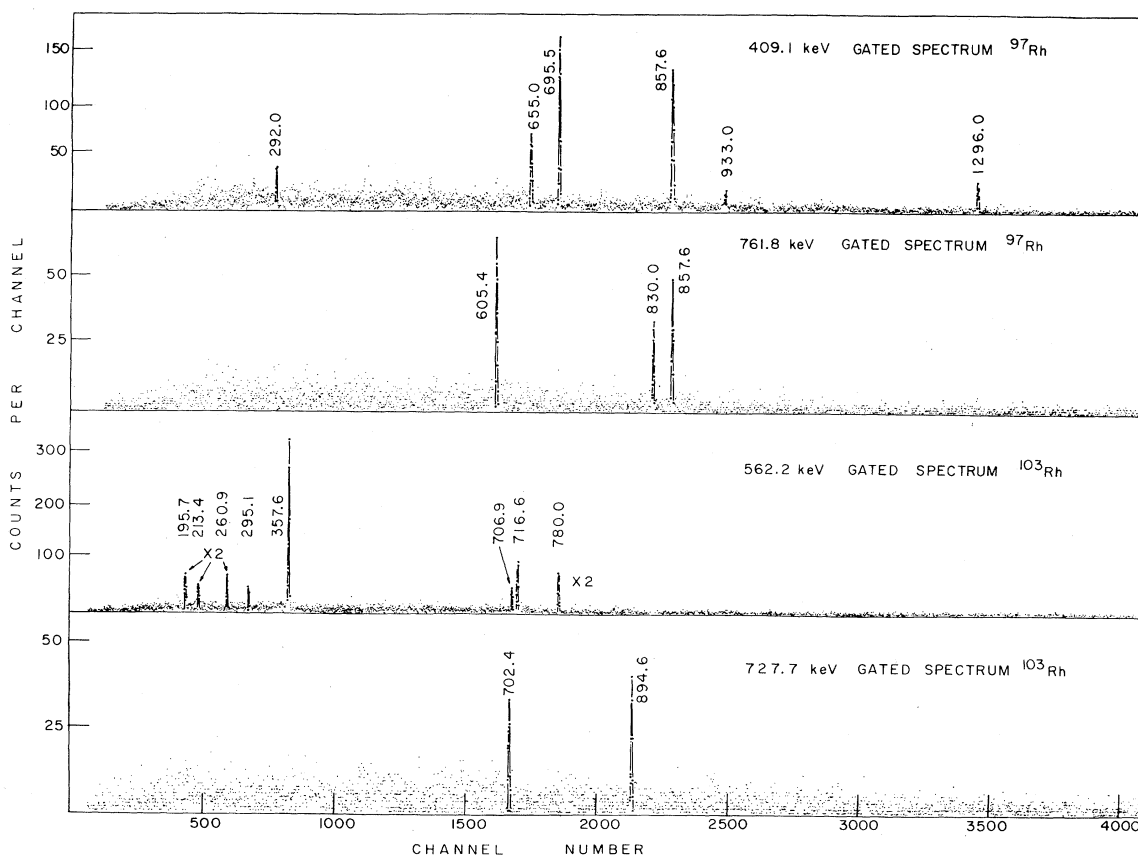


FIG. 2. Some examples of γ - γ coincidence spectra obtained in this work for transitions in ⁹⁷Rh and ¹⁰³Rh. Energies are in keV.

TABLE I. A summary of level energies, gamma-ray energies, relative intensities, and angular distribution results for ^{97}Rh obtained in this work. Energies are in keV.

Excitation energy (keV)	γ -ray energy (keV)	Relative intensity (%)	$J_i^\pi \rightarrow J_f^\pi$	A_2	A_4	δ
						$E2/M1$
857.6	857.6	100.	$\frac{13}{2}^+ \rightarrow \frac{9}{2}^+$	0.255	-0.103	$E2$
1463.0	605.4	36.6 ± 1.5	$(\frac{15}{2}, \frac{11}{2})^\pm \rightarrow \frac{13}{2}^+$	-0.093 ± 0.061	-0.018 ± 0.062	
1553.1	695.5	50.4 ± 1.5	$(\frac{17}{2}, \frac{13}{2})^+ \rightarrow \frac{13}{2}^+$	0.253 ± 0.048	-0.105 ± 0.054	
1962.2	409.1	33.1 ± 1.0	$(\frac{19}{2}, \frac{15}{2})^+ \rightarrow (\frac{17}{2}, \frac{13}{2})^+$	-0.207 ± 0.039	0.009 ± 0.041	$M1$
2224.8	761.8	22.8 ^a ± 1.5	$\rightarrow (\frac{15}{2}, \frac{11}{2})^\pm$			
2617.2	655.0					
3054.8	830.0					
3258.2	1296.0					
3550.2	292.0					
	933.0					

^aDoublet-total intensity only.

The yields of all reaction gamma rays in each spectrum were obtained with the peak-fitting program SAMPO.⁶ Relative excitation functions of transitions attributed to ^{97}Rh and ^{103}Rh were drawn to obtain an estimate of the spin of a particular level. These spin values were then used to fit the angular distribution data following procedures which are well documented and will not be repeated here.^{7,8}

A. Results for ^{97}Rh

The results obtained for ^{97}Rh are summarized in Table I, while the corresponding decay scheme is shown in Fig.

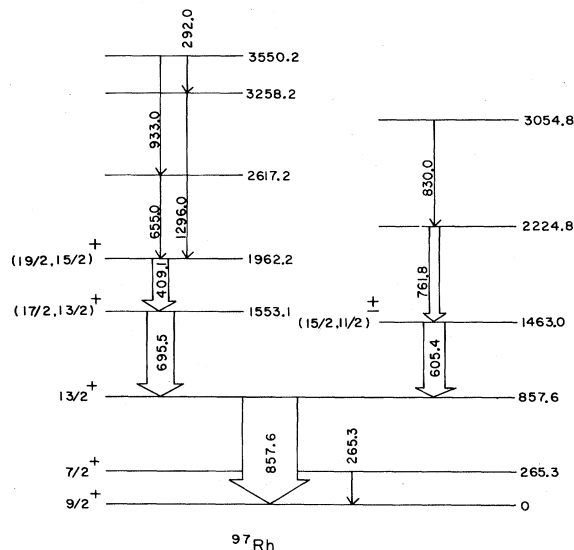


FIG. 3. Level scheme of ^{97}Rh as obtained in this work. Energies are in keV. Spins in parentheses are probable, but not definitively established. Dotted transitions and levels are the most probable placements.

3. Examples of the excitation function data are shown in Fig. 4.

Previous work on the decay of ^{97}Pd has established⁵ many levels in ^{97}Rh which were not or were only weakly excited in this study. The $\frac{7}{2}^+$ level at 265.3 keV could not be verified from our work, although the excitation function of the 265.3 keV gamma ray observed in our spectra would support a $\frac{7}{2}$ spin assignment (Fig. 4). The $\frac{5}{2}^+$ level observed at 475.1 keV was not excited in this

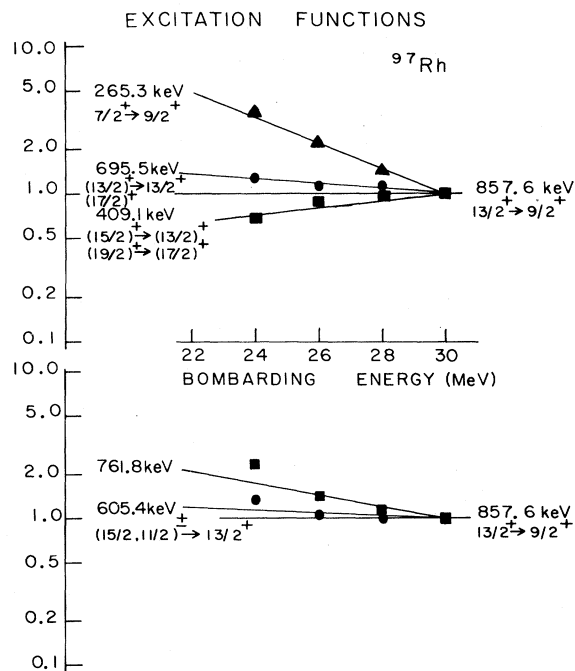


FIG. 4. Relative excitation functions of transitions in ^{97}Rh . The yield of each gamma ray is normalized to that of the 857.6 keV line.

work, and we have little evidence for the ($\frac{3}{2}^{-}, \frac{5}{2}^{-}$) level at 1004.8 keV. The 745.7 keV transition observed to deexcite the 1004.8 keV level in decay work can be entirely attributed in our work to ^{98}Ru populated via the $^{6}\text{Li}, \text{pn}$ reaction. The many additional levels attributed to ^{97}Rh from decay work could not be confirmed from our data.

A strong 857.6 keV transition was found to be in coincidence with several gamma rays, none of which could be identified with the various possible reaction product nuclei, and we place the 857.6 keV transition as deexciting to the ground state of ^{97}Rh . The predominantly quadrupole nature of the 857.6 keV transition as deduced from its angular distribution favors a $\frac{13}{2}^{+}$ spin-parity assignment to the level at 857.6 keV.

Additional levels built on the 856.7 keV state could be deduced from the gamma-gamma coincidence data. The 857.6-605.4-761.8-830.0 keV coincidences necessitate levels at 1463.0, 2224.8, and 3054.8 keV, respectively. We can say little on the 3054.8 and 2224.8 keV levels since their deexcitation gamma rays are both doublets. The excitation function of the 605.4 keV transition favors a spin of around $\frac{13}{2}$, while its almost isotropic angular distribution would support $\frac{15}{2}$ or $\frac{11}{2}$. We cannot distinguish between these two possibilities. Also, we cannot rule out a negative parity to the 1463.0 keV level, although it is unlikely since even a small $M2$ component in the 605.4 keV transition would result in a long (~ 10 ns) lifetime for the 1463.0 keV level. The strong 605.4-761.8 keV coincidence would suggest an almost pure $E1$ transition in the case of a change in parity.

A second cascade of transitions is built on the 857.6 keV level, as shown in Fig. 3. Only the 695.5 and 409.1 keV transitions were intense enough to enable some estimate of the spins to be made. In addition, the ordering of the 655.0 and 933.0 keV transitions may be reversed. The angular distribution of the 695.5 keV γ ray shows it to be a predominantly quadrupole transition favoring a $\frac{17}{2}, \frac{13}{2}$, or $\frac{9}{2}$ spin value for the 1553.1 keV level. Its excitation function supports a $\frac{13}{2}$ value, but from the level systematics (see Sec. III), the $\frac{17}{2}$ spin should not be ruled out. Lifetime considerations favor a positive parity. The excitation function and angular distribution of the 409.3 keV transition would then imply a $\frac{19}{2}$ or $\frac{15}{2}$ spin for the level at 1962.2 keV.

B. Results for ^{103}Rh

The results obtained for ^{103}Rh are summarized in Table II, while the corresponding decay scheme is shown in Fig. 5. Some excitation functions of particular relevance are shown in Fig. 6. We discuss negative and positive parity levels separately.

1. Negative parity levels:

295.1, 357.6, 847.6, 877.9, and 919.8 keV levels

Previous work has already established¹ a $\frac{3}{2}^{-}, \frac{5}{2}^{-}$ doublet of levels at 295.1 and 357.6 keV, respectively, with transitions to the $\frac{1}{2}^{-}$ ground state. This is completely in

agreement with our data on the two ground state transitions. We have some evidence for an additional low spin state at 847.6 keV. A level at 847.7 keV has been observed in Coulomb excitation work⁹ with a tentative $\frac{7}{2}^{-}$ spin-parity assignment.¹⁰ Our angular distributions on the known 490.9 and 522.3 keV transitions to the $\frac{5}{2}^{-}$ and $\frac{3}{2}^{-}$ levels, respectively, favor a $\frac{3}{2}$ or $\frac{7}{2}$ spin assignment with the former clearly favored by the excitation function data. Interestingly enough, in a previous work² on ^{101}Rh a similar level at 850.4 keV was observed for which a $\frac{3}{2}$ spin assignment was favored as opposed to the $\frac{7}{2}$ value proposed in a p,t pickup reaction study.¹¹ Of the additional levels observed in previous work only the 919.8 keV, $\frac{9}{2}^{-}$ level was detected here. The $\frac{9}{2}$ spin assignment¹⁰ is completely consistent with our data on the 562.2 keV transition deexciting the level to the $\frac{5}{2}^{-}$, 357.6 keV state. The existence of a 877.9 keV level is inferred here from the weak 530.3-357.6 keV coincidence. The limited data available on the 530.3 keV transition would suggest a spin $\frac{1}{2}$ or $\frac{3}{2}$ assignment to this level with negative parity from its decay mode.

2. 1636.4, 2343.3, and 2416.4 keV levels

The 357.6 and 562.2 keV transitions are in strong coincidence with 716.6, 706.9, and 780.0 keV lines. In addition, the 706.9 and 780.0 keV transitions are not in coincidence with each other, although the 780.0 keV transition is in coincidence with the 716.6-562.2-357.6 keV cascade. This necessitates new levels at 1636.4, 2343.3, and 2416.4 keV. The predominantly quadrupole nature of the 716.6 and 706.9 keV transitions and their respective excitation functions favor $\frac{13}{2}^{-}$ and $\frac{17}{2}^{-}$ spin-parity assignments to the levels at 1636.4 and 2343.3 keV, respectively. The angular distribution of the 780.0 keV transition also has a predominantly quadrupole character favoring a $\frac{17}{2}$ spin assignment to the 2416.4 keV level. The excitation function of the 780.0 keV transition is consistent with this assignment, although its behavior suggests that it could be a doublet (Fig. 6).

3. 2539.1, 2752.5, 3013.4, and 3329.3 keV levels

Four low-energy transitions were detected in coincidence with the 706.9, 716.6, 562.2, and 357.6 keV transitions suggesting levels at 2539.1, 2752.5, 3013.4, and 3329.4 keV. The angular distributions of all four transitions are almost identical, being predominantly of a $\Delta J=1$ nature. The level ordering is not unambiguously determined from the γ - γ coincidence data. We have placed the levels in order of increasing spin value as determined from the excitation function data.

4. Positive parity levels:

536.9, 657.1, and 820.7 keV levels

Low-lying $\frac{7}{2}^{+}$ and $\frac{9}{2}^{+}$ states at 40.0 and 93.0 keV, respectively, have been observed in ^{103}Rh .¹² A level at 536.9 keV is strongly populated in the decay of ^{103}Ru (Ref. 13) and has also been observed in p,p' scattering experiments.¹⁴ The $\frac{5}{2}^{+}$ spin-parity assignment from these

TABLE II. A summary of level energies, γ -ray energies, relative intensities, and angular distribution results for ^{103}Rh obtained in this work. Energies are in keV.

Excitation energy (keV)	γ -ray energy (keV)	Relative intensity (%)	$J_i^\pi \rightarrow J_f^\pi$	A_2	A_4	δ $E2/M1$
295.1	295.1	32.9±0.4	$\frac{3}{2}^- \rightarrow \frac{1}{2}^-$	-0.186 ±0.016	0.011 ±0.018	
357.6	357.6	100	$\frac{5}{2}^- \rightarrow \frac{1}{2}^-$	0.167 ±0.007	-0.061 ±0.010	E2
536.9	497.0	14.9±1.0	$\frac{5}{2}^+ \rightarrow \frac{7}{2}^+$	0.041 ±0.027	-0.049 ±0.033	
657.1	564.1	54.2±0.5	$\frac{11}{2}^+ \rightarrow \frac{9}{2}^+$	0.223 ±0.015	-0.024 +0.021	
	617.2	5.4±0.2	$\rightarrow \frac{7}{2}^+$	0.160 ±0.038	-0.027 ±0.046	E2
820.7	163.9	9.5±0.3	$\frac{13}{2}^+ \rightarrow \frac{11}{2}^+$	-0.175 ±0.039	0.003 ±0.045	M1
	727.7	79.3±0.8	$\rightarrow \frac{9}{2}^+$	0.225 ±0.017	-0.087 ±0.022	E2
847.6	490.0	11.2±0.4	$(\frac{3}{2}^-) \rightarrow \frac{5}{2}^-$	-0.219 ±0.041	0.035 ±0.046	
	552.3	5.1±0.4	$\rightarrow \frac{3}{2}^-$	0.101 ±0.081	-0.082 ±0.097	
887.9	530.3	4.8±0.3	$(\frac{3}{2}, \frac{1}{2})^- \rightarrow \frac{5}{2}^-$	0.095 ±0.081	0.012 ±0.059	
919.8	562.2	76.0±0.8	$\frac{9}{2}^- \rightarrow \frac{5}{2}^-$	0.212 ±0.015	-0.083 ±0.019	E2
1348.9	691.8	14.7±0.4	$(\frac{13}{2}^+) \rightarrow \frac{11}{2}^+$	0.321 ±0.028	0.018 ±0.034	-0.9 $^{+0.4}_{-0.6}$
1519.7	862.6	18.2±0.6	$(\frac{11}{2}, \frac{9}{2})^+ \rightarrow \frac{11}{2}^+$	0.189 ±0.024	0.061 ±0.031	
1523.1	702.4	14.5±0.4	$\frac{15}{2}^+ \rightarrow \frac{13}{2}^+$	0.139 ±0.028	0.011 ±0.034	
	866.3	7.5±0.2	$\rightarrow \frac{11}{2}^+$	0.272 ±0.037	-0.123 ±0.049	E2
1636.4	716.6	49.1±0.5	$\frac{13}{2}^- \rightarrow \frac{9}{2}^-$	0.240 ±0.007	-0.098 ±0.096	E2
1715.3	894.6	27.8±0.5	$\frac{17}{2}^+ \rightarrow \frac{13}{2}^+$	0.228 ±0.030	-0.094 ±0.035	E2
2194.9	846.0	7.1±0.3	$\rightarrow (\frac{13}{2}^+)$	0.246 ±0.061	-0.006 ±0.074	
2343.3	706.9	16.5±0.3	$(\frac{17}{2}^-) \rightarrow \frac{13}{2}^-$	0.250 ±0.022	-0.096 ±0.028	E2
2416.4	780.0	9.8±0.5	$(\frac{17}{2}^-) \rightarrow \frac{13}{2}^-$	0.245 ±0.037	-0.087 ±0.048	E2
2539.1	195.8	15.3±0.3	$(\frac{19}{2}^-) \rightarrow (\frac{17}{2}^-)$	-0.146 ±0.015	0.018 ±0.017	M1
2736.3	1021.0	5.8±0.3	$(\frac{21}{2}^+) \rightarrow \frac{17}{2}^+$	0.312 ±0.060	-0.144 ±0.077	E2
2752.5	213.4	14.3±0.3	$(\frac{21}{2}^-) \rightarrow (\frac{19}{2}^-)$	-0.169 ±0.014	0.004 ±0.015	M1
3013.4	260.9	5.8±0.3	$(\frac{23}{2}^-) \rightarrow (\frac{21}{2}^-)$	-0.124 ±0.050	-0.044 ±0.058	M1
3329.3	315.9	2.8±0.2	$(\frac{25}{2}^-) \rightarrow (\frac{23}{2}^-)$	-0.161 ±0.068	0.041 ±0.074	M1

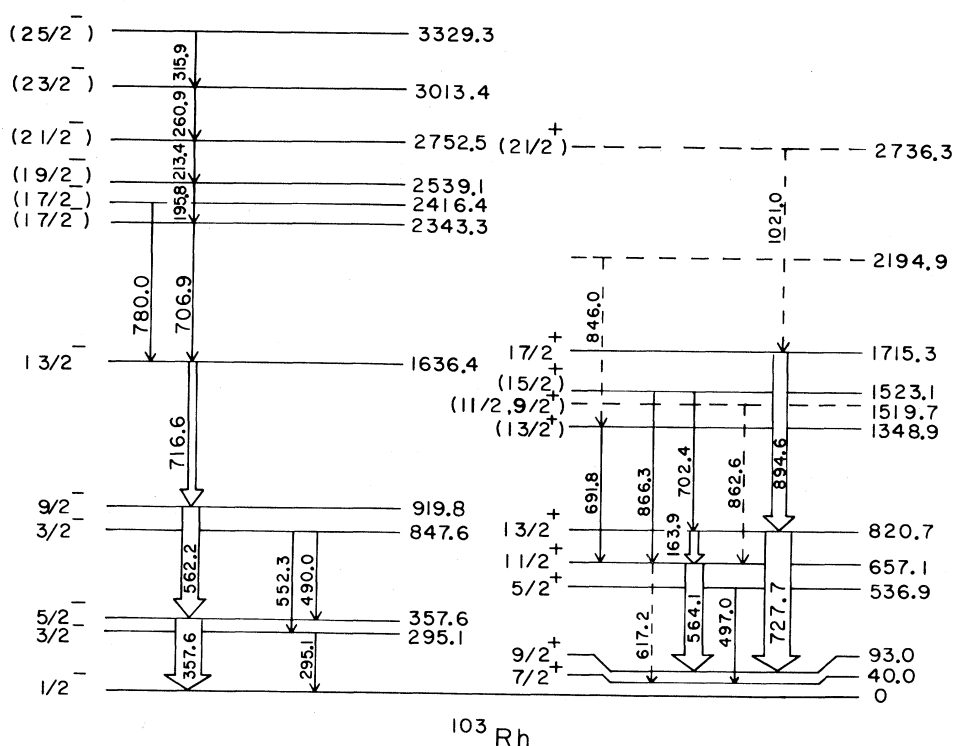


FIG. 5. Level scheme of ^{103}Rh as obtained in this work. Same caption as Fig. 3.

studies is consistent with our data on the 497.0 keV transition deexciting it to the $7/2^+$, 40.0 keV level. Other low-lying levels seen in decay work were not excited in this study and we can say little about the levels at 607.7, 650.1, and 651.8 keV.

A search was made for possible transitions to the $9/2^+$ and $7/2^+$ states. In this we were guided by previous work on ^{101}Rh ,² and we looked specifically for transitions with similar excitation functions to those observed in the negative-parity band. Strong lines at 564.1 and 727.7 keV, which could not be identified with any of the expected product nuclei, have the correct shapes in their excitation functions, and we propose that they feed the $9/2^+$ level at 93.0 keV, forming levels at 657.1 and 820.7 keV, respectively. The excitation function data on the 727.7 keV transition favors a $13/2^-$ spin assignment, which is further supported by the predominantly quadrupole nature of the 727.7 keV transition as deduced from its angular distribution. An $11/2^-$ spin is favored from the excitation function and angular distribution of the 564.1 keV transition. We have some evidence for a 163.9 keV transition between the 657.1 and 820.7 keV states. The 163.9 keV gamma ray appears weakly in the coincidence spectrum, but its gated spectrum clearly shows the presence of the 564.1 keV line. Its excitation function is identical to that of the 727.7 keV transition, while its angular distribution is well fitted to a $\Delta J=1$ transition.

5. 1348.9, 1519.7, 1523.1, and 1715.3 keV levels

The level at 1348.9 keV is inferred from the 691.8-564.1 keV coincidence. The excitation function of the 691.8 keV transition is identical to that of the 727.7 keV gamma ray, and a $13/2^-$ spin is not inconsistent with the angular distribution data.

Our evidence for the level at 1519.7 keV is very weak and is based on the weak 862.6-564.1 keV coincidence. An $11/2^-$ or $9/2^-$ spin is possible from the excitation function data. The angular distribution does not distinguish between these two possibilities.

A level at 1523.1 keV is firmly established via the 866.3-564.1 and 702.4-727.7 keV coincidences. The excitation functions of the 866.3 and 702.4 keV transitions suggest a spin $\approx 13/2^-$, while the angular distribution data strongly favor a $15/2^-$ spin assignment.

A very weak 617.2 keV line appears in the 866.3 keV gated spectrum and may deexcite the $11/2^+$, 657.1 keV level to the isomeric $7/2^+$ state. Our data on the 617.2 keV transition are consistent with an $11/2^+$ spin assignment to the level at 657.1 keV, and its weakness shows that a precise trend exists in these nuclei since in ^{101}Rh no $11/2^+$ to $7/2^+$ transition was observed.

The strong 894.6-727.7 keV coincidence establishes a level at 1715.3 keV. A $17/2^+$ spin assignment is strongly favored by the excitation function data (Fig. 6) and the

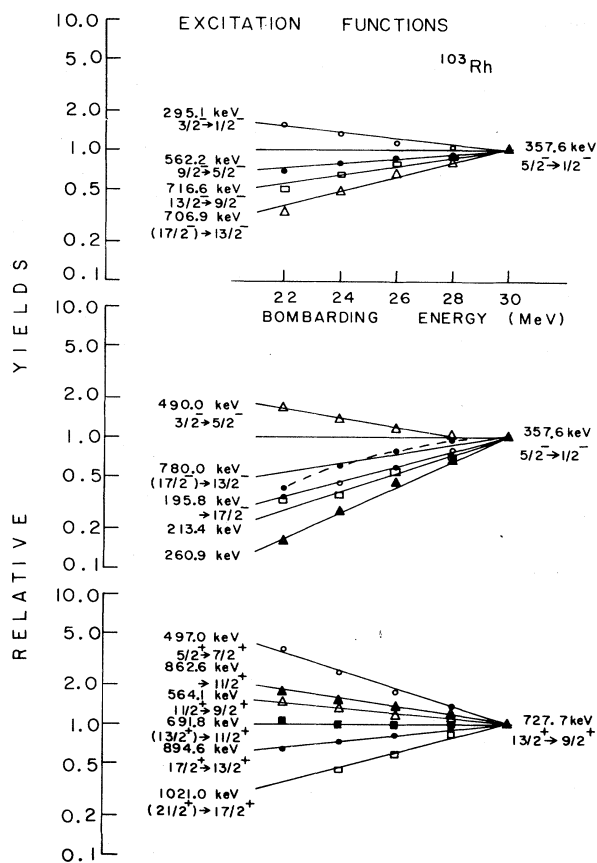


FIG. 6. Relative excitation functions of transitions in ^{103}Rh . The yields of transitions from levels with probable negative parity are normalized to that of the 357.6 keV line, while the yields of transitions deexciting probable positive parity levels are normalized to that of the 727.7 keV gamma ray.

predominantly quadrupole nature of the 894.6 keV transition.

6. 2194.9 and 2736.3 keV levels

We can say little about the level at 2194.9 keV which is based on the weak 846.0-691.8 keV coincidence. The gated spectrum of the 1021.0 keV transition shows weak coincident lines at 894.6 and 727.7 keV, suggesting a level at 2763.3 keV. Its excitation function (Fig. 6) and angular distribution strongly favor a $\frac{21}{2}$ spin assignment.

III. DISCUSSION AND CONCLUSION

The ^{97}Rh nucleus, with five protons outside the semi-closed shell of 40 protons and only two neutrons outside the magic shell of 50 neutrons, could be expected to be largely characterized by shell model wave functions and/or by the phonon-coupling model. Indeed, shell model calculations have been reported for ^{95}Rh ($N=50$, Ref. 15), and good agreement between experiment and theory was achieved for the level energies and spins. However, no such calculations have yet been reported for ^{97}Rh . From a cursory inspection of the present data on

^{97}Rh and ^{95}Rh ,¹⁶ it appears clear that both nuclei have some similarities which differentiate them from the other more neutron-rich Rh nuclei. For instance, both ^{95}Rh and ^{97}Rh have $\frac{9}{2}^+$ ground states, whereas from ^{99}Rh to ^{103}Rh the ground state is $\frac{1}{2}^-$ and becomes $\frac{7}{2}^+$ in ^{105}Rh . Moreover, both nuclei are characterized by a strongly excited $\frac{13}{2}^+$ state and the apparent absence of a strong negative-parity band. In evaluating our data on ^{97}Rh , however, we are hindered by the lack of unambiguous spin assignments to the levels above the $\frac{13}{2}^+$, 857.6 keV state and our discussion must be somewhat speculative. The position of the $\frac{13}{2}^+$ state fits in well with the level systematics of the $\frac{13}{2}^+$ states in the odd mass Rh nuclei^{1,2,16} and lies close to the 2^+ state at 832.3 keV in ^{96}Ru . A $\frac{17}{2}^+$ level at 1553.1 keV would also fit in well, lying close to the 4^+ state in ^{96}Ru at 1516.9 keV. A $\frac{15}{2}^+$ assignment to the level at 1463.0 keV would be surprising. In the isotope ^{95}Tc the $\frac{15}{2}^+$ state is observed above the $\frac{17}{2}^+$ state, as it is in ^{93}Tc and ^{97}Tc . This level ordering is reversed in ^{101}Rh (Ref. 2) and probably also in ^{99}Tc . No $\frac{15}{2}^+$ state has been observed in ^{99}Rh .² We can say little on the higher lying levels in ^{97}Rh , and clearly, additional experimental work is needed.

From the available experimental data clear patterns seem to emerge in the mass region A around 100. For instance, in the even-even $N=54, 56,$ and 58 isotones, the energy of the first excited 2^+ state shows a minimum at around $Z=45$, while the ratios of the energies of the first 4^+ and 2^+ states show a maximum around the same value. This might reflect some movement away from a spherical shape between $Z=40$ and 50 . For $N=60$, however, there is no minimum in the 2^+ excitation energy between $Z=40$ and 50 whereas the 4^+ to 2^+ ratio of energies shows large variations with Z , with the maximum approaching the pure rotor value. This may be suggestive of a move to a deformed shape at $N=60$. A similar pattern should also be present in the odd-even nuclei of Tc ($Z=43$) and Rh ($Z=45$) with the turning points at $^{101,103}\text{Tc}$ and $^{103,105}\text{Rh}$ ($N=58$ and 60 , respectively). Indeed, De Gelder *et al.*⁴ have proposed the onset of a stable quadrupole deformation at $N=58$ and 60 for the Tc isotopes. Their calculations, based on the interacting boson-fermion model (IBFM), reproduce very well the $\frac{5}{2}^+$, $\frac{7}{2}^+$, and $\frac{9}{2}^+$ level ordering that they observed in ^{103}Tc via the $^{104}\text{Ru}(d, ^3\text{He})$ reaction. Together with the $\frac{11}{2}^+$ and $\frac{13}{2}^+$ states, these levels would then form a rotational-like band. Clearly a similar structure should be observable in ^{105}Rh . However, the available data on ^{105}Rh (Ref. 1) and the present results on ^{103}Rh are not conducive to a similar interpretation. The level structure of ^{103}Rh , as unveiled in this study, fits in well with the level systematics of the other odd-mass Rh nuclei.^{1,2} The splitting between the $\frac{17}{2}^+$ and $\frac{15}{2}^+$ states and the $\frac{13}{2}^+$ and $\frac{11}{2}^+$ states is slightly larger in ^{103}Rh than in ^{101}Rh . However, the positions of these levels in ^{103}Rh lie close to the observed states in ^{101}Rh . Furthermore, the $\frac{11}{2}^+$, $\frac{13}{2}^+$, $\frac{15}{2}^+$, and $\frac{17}{2}^+$ level energies in ^{105}Rh do not seem substantially lower, and while the ground state of ^{105}Rh is $\frac{7}{2}^+$, no

close-lying $\frac{5}{2}^{+}$ level has yet been reported. (The lowest observed $\frac{5}{2}^{+}$ state is at 499 keV.) Strangely enough, a $\frac{5}{2}^{+}$ ground state has been proposed¹ for ^{107}Rh , about which very little is presently known. Clearly all this seems to indicate that there is no sudden move to a deformed shape in the $^{103,105}\text{Rh}$ nuclei. This is also suggested by the available data on the negative-parity band structure. The positions of the $\frac{5}{2}^{-}$, $\frac{9}{2}^{-}$, and $\frac{13}{2}^{-}$ states show little movement between ^{99}Rh and ^{105}Rh , while the $\frac{3}{2}^{-}$, $\frac{5}{2}^{-}$ doublet of states shows only a very small splitting suggestive more of a vibrational weak-coupling picture where negative parity states arise from the coupling of a $2p_{1/2}$ proton (or hole) to the phonon excitation states of the core. No detailed calculations in this framework have been carried out for the odd-mass Rh nuclei. The very same model is only moderately successful in describing the odd-even Tc nuclei.¹⁷

Calculations in the vibrational limit [SU(5)] of the IBFM are beginning to be performed in this region with encouraging results. The work of De Gelder *et al.*⁴ was already mentioned above in connection with ^{103}Tc and the onset of deformation at $N=58$ and 60. Kaup *et al.*¹⁸

have obtained very good agreement with experiment for the positive-parity states in ^{97}Tc , ^{105}Ag , and ^{107}Ag . The calculations done by these authors coupled one odd proton in the $g_{9/2}$ particle state to the boson core. Vervier and Janssens¹⁹ couple a $p_{1/2}$ proton to a ^{102}Ru boson core and reproduce very well the low-lying $\frac{5}{2}^{-}$, $\frac{3}{2}^{-}$ doublet of states and the $\frac{9}{2}^{-}$, $\frac{7}{2}^{-}$, $\frac{5}{2}^{-}$, and $\frac{3}{2}^{-}$ excited states in ^{103}Rh . It would be interesting to have similar calculations carried out in a systematic manner also for the other odd-mass Rh and Tc nuclei. Even if enough experimental data are now available on these nuclei to spur a deeper and more systematic development of such calculations, it is felt that additional experimental work is still needed for a better understanding of the nuclear structure of the neutron-rich Tc and Rh isotopes.

ACKNOWLEDGMENTS

The authors wish to thank the technical and scientific staff of the Chalk River Nuclear Laboratories for their aid in the data acquisition and data reduction procedures. This work was supported by the Natural Science and Engineering Research Council of Canada.

*Present address: Division of Physics, National Research Council, Ottawa, Ontario, Canada K1A 0R6.

¹Tables of Isotopes, 7th ed., edited by C. M. Lederer and V. S. Shirley (Wiley, New York, 1978), pp. 372–457.

²G. Kajrys, M. Irshad, S. Landsberger, R. Lecomte, P. Paradis, and S. Monaro, Phys. Rev. C **26**, 138 (1982).

³G. Kajrys, M. Irshad, S. Landsberger, R. Lecomte, P. Paradis, and S. Monaro, Phys. Rev. C **26**, 1462 (1982).

⁴P. De Gelder, D. de Frenne, K. Heyde, N. Kaffrell, A. M. Van den Burg, N. Blasi, M. N. Harakeh, and W. A. Sterrenburg, Nucl. Phys. **A401**, 397 (1983).

⁵H. Götürk, N. K. Aras, P. Fettweiss, P. Del Marmol, J. Vanhorenbeeck, and K. Cornelis, Nucl. Phys. **A344**, 1 (1980).

⁶J. T. Routti and S. G. Poussin, Nucl. Instrum. Methods **72**, 125 (1969).

⁷P. Taras and B. Haas, Nucl. Instrum. Methods **123**, 73 (1975).

⁸G. Kajrys, S. Landsberger, R. Lecomte, and S. Monaro, Phys. Rev. C **27**, 983 (1983).

⁹J. L. Black, W. J. Caelli, and R. B. Watson, Nucl. Phys. **A125**, 545 (1969).

¹⁰R. O. Sayer, J. K. Temperley, and D. Eccleshall, Nucl. Phys. **A179**, 122 (1972).

¹¹R. M. Del Vecchio, R. A. Naumann, J. R. Duran, H. Hübel, and W. W. Daehnick, Phys. Rev. C **12**, 69 (1975).

¹²D. C. Kocher, Nucl. Data Sheets **13**, 343 (1974).

¹³W. H. Zoller, E. S. Macias, M. B. Perkad, and W. B. Walters, Nucl. Phys. **A130**, 293 (1969).

¹⁴J. L. Black, W. J. Caelli, and R. B. Watson, Nucl. Phys. **A125**, 545 (1969).

¹⁵A. Amusa and R. D. Lawson, Z. Phys. A **307**, 333 (1982).

¹⁶E. Nolte, G. Korschinek, and U. Hein, Z. Phys. A **298**, 191 (1980).

¹⁷Chr. Bargholtz and S. Beshai, Z. Phys. A **283**, 89 (1977).

¹⁸U. Kaup, R. Vorwerk, D. Hippe, H. W. Schuh, P. von Brentano, and O. Scholten, Phys. Lett. **B106**, 439 (1981).

¹⁹J. Vervier and R. V. F. Janssens, Phys. Lett. **B108**, 1 (1982).